

# Ion Beam Time-of-Flight Mass-to-Charge Analyzer for Ion Implantation Facility<sup>1</sup>

V.I. Gushenets, A.G. Nikolaev, L.G. Vintzenko, E.M. Oks,  
G.Yu. Yushkov, A. Oztarhan,\* and I.G. Brown\*\*

*High Current Electronics Institute, Russian Academy of Sciences, 4 Academichesky ave.,  
Tomsk, 634055, Russia, Ph: +7 (3822) 491776, Fax: +7 (3822) 492410, E-mail: nik@opee.hcei.tsc.ru*

*\* Ege University, Bornova-Izmir, 35100 Turkey*

*\*\* Lawrence Berkeley National Laboratory, Berkeley, California 94720, USA*

**Abstract – We describe the design, electronics, and test results of a time-of-flight ion beam mass-to-charge analyzer for ion implantation facility that is used for ion beam material modification. The method selects a short-time sample of the beam whose mass-to-charge composition is then separated according to ion velocity and detected by a remote Faraday cup. The analyzer is a detachable device that can be used for rapid analysis of mass-to-charge composition of ion beams accelerated by voltages of up to about 100 kV.**

## 1. Introduction

Ion beams in the energy range of about 5 to 100 keV are employed widely for fundamental studies and for a variety of technological applications for ion beam material modification [1–3]. Magnetic spectrometry [4] is often used for measuring the mass-to-charge ( $M/q$ ) composition of such beams. The method is based on the deflection of ions in a transverse magnetic field and has high resolution and reasonable sensitivity. In this analytical approach the beam is coupled to the magnetic spectrometer *in toto* and at all times – that is, the beam is not sampled but is continuously analyzed. Thus this method is rather elaborate, consumes significant energy, is not low cost, and the beam cannot be used for its primary purpose while the analysis is taking place. While for many situations these constraints are acceptable and magnetic  $M/Q$  analysis is the preferred approach, for other situations an alternative method may be more suitable.

The time-of-flight (TOF) method for measuring the mass-to-charge composition of an ion beam is based on the different times required for ions of different  $M/Q$  values to drift over a fixed distance, and requires analysis of only a small time-sample of the ion beam that is deflected from its initial path [2, 3, 5, 6]. The time-of-flight spectrometer possesses a reasonably high resolving power,  $(M/Q)/\Delta(M/Q) > 10$ , and a

rather high sensitivity, allowing analysis of ions from hydrogen to uranium. Analysis of all beam components is done at the same time. As for many ion beam techniques, there are constraints on the vacuum chamber pressure, which should be less than  $\sim 10^{-4}$  Torr since scattering of the ion beam by residual gas atoms and the associated energy loss during the ion drift time should be minimal. Since this is precisely the operating pressure regime that is typical of most ion sources and ion beam applications, this is usually not a burden [6].

The investigation of mass-to-charge composition of ion beams by the time-of-flight method has been used extensively in studies utilizing the MEVVA [7], TITAN [8, 9] and other [10] vacuum arc ion sources. Modification of this kind of time-of-flight spectrometer has allowed us to increase the resolution and decrease the distortion of ion current signals [9].

Here we describe a modified, detachable time-of-flight mass spectrometer that can be installed easily for analysis of ion beam mass-to-charge composition, and present the results of  $M/q$  measurements of the ion beam generated by the MEVVA-V vacuum arc ion source at Izmir, Turkey. Detailed consideration is given to the design and operating principles of the analyzer, and to the electronic circuitry.

## 2. Design and Principle of Operation

The overall layout of the time-of-flight analyzer is shown in Fig. 1. The analyzer system is housed in a stainless steel vessel 1, through which the ions drift, of length 1 m and diameter 25 cm. The spectrometer gate 2, is located at the beam entrance end of the vessel, and a Faraday cup 3, at the other end. The gate of the analyzer (Fig. 2) consists of five pairs of concentric metallic rings or plates (short sections of tubes – the rings have axial length) spaced 1 cm apart. For each pair of rings, the outer ring is grounded and the inner is connected to electronics that provides an ion-

<sup>1</sup> The work was supported by:

- U.S. Department of Energy, Initiatives of Proliferation Prevention, project IPP-LBNL-T2-196, under Contract No. DE-AC03-76SF00098;
- Grant of the President of the Russian Federation, the Dr. Sci. Program MD-148.2203.02;
- US Civilian Research and Development Foundation, under Grant No. TO-016-02.

deflecting voltage pulse of variable amplitude  $V_{\text{defl}} = 1\text{--}5\text{ kV}$  and duration  $\tau \leq 100\text{ ns}$ . The axial length of each deflection ring increases with radius to allow for the greater deflection that is required for ions at greater radius; see below. The central part of the gate is a flat metal plate of diameter 5 cm that blocks the direct passage of the ion beam into the Faraday cup; this plate can serve double-duty as a monitor of ion beam current (without secondary electron suppression, so the measurement is relative and approximate). The gating-plate array should be accurately on-axis with respect to the ion source and ion beam trajectory and perpendicular to the axis. For this purpose we allowed for manipulation of the gate array through an angle of up to  $15^\circ$  by means of a gimbaled suspension mechanism [11]. The Faraday cup inlet aperture is 1 m in diameter. To preclude distortion of the ion current signal due to secondary electron emission from the collector [12], secondary electrons are suppressed by a transverse magnetic field of  $\sim 40\text{ mT}$  in the region just in front of the Faraday cup collector by a pair of SmCo permanent magnets. The unit is attached to the main vacuum chamber so as to allow entrance of the ion beam in a direction perpendicular to the plane of the spectrometer gate.

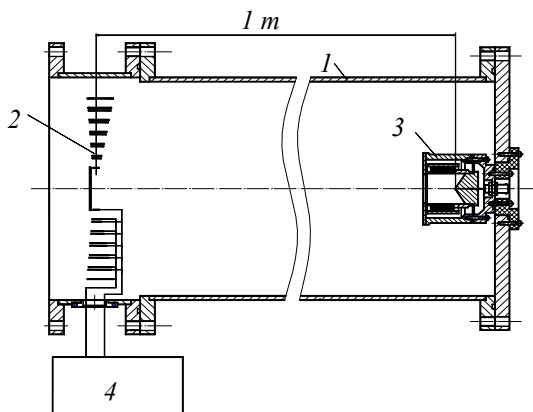


Fig. 1. Simplified schematic of the overall time-of-flight analyzer system: 1 – vacuum chamber; 2 – nested gating plate array; 3 – Faraday cup detector, 4 – pulse generator



Fig. 2. Gating plate array (left) and magnetically insulated Faraday cup (right)

The electronics provides an ion deflection pulse to each pair of gating plates. The electric field formed between the plates deflects the ions from their initial path through an angle  $\theta$  as required for them to be redirected to the Faraday cup entrance aperture. The ion beam deflection (small angle approximation) is given by

$$\text{tg}\theta = V_{\text{defl}} / 2dV_{\text{accel}}, \quad (1)$$

where  $V_{\text{defl}}$  is the deflection pulse amplitude,  $V_{\text{accel}}$  is the ion source extraction voltage,  $l$  is the axial length of the gating plates, and  $d$  is radial separation of the gating plates (separation between the two plates of a pair). Note that the angle of deflection  $\theta$  does not depend on the ion  $M/Q$  ratio. The deflection angle  $\theta$  needs to be greater for ions near the periphery of the beam than for ions closer to the beam axis. For this reason the rings of larger diameter were made to be of greater axial length  $l$  also. At the same time, the ring length  $l$  was chosen to be less than the drift distance of the slowest ions ( $U^+$  ions) in a time period equal to the deflection pulse duration  $\tau$ .

We point out here that the time-of-flight approach is based on the assumption that all ions subject to analysis have reached their final energy by acceleration through the same fixed potential drop. This is the case for an ion beam formed by an ion source, for which all ions in the beam have energy given by  $\frac{1}{2}Mv^2 = qV_{\text{accel}}$ . However this is not always the case, as for example for ions accelerated in a drift tube accelerator, when all ions have the same velocity and hence a time-of-flight approach is not appropriate.

Because the deflection pulse duration  $\tau$  is much less than the time  $t$  for ions to drift the total distance  $L$  from the gating plates to the Faraday cup (the spectrometer base), a short beam packet is selected containing ions that drift toward the Faraday cup detector. The drift time  $t$  is given by

$$t = L(M/Q)^{1/2} (2eV_{\text{accel}})^{-1/2}, \quad (2)$$

where now we distinguish between the ion charge  $q$  and its charge state  $Q$ , with  $q = eQ$  and  $e$  is (the magnitude of) the electronic charge. The drift time  $t$  given above is  $M/Q$ -dependent. Thus the short beam packet selected by the gating plates separates in its drift into the various  $M/Q$  components present in the beam. When the Faraday cup signal is observed on an oscilloscope, peaks are observed at times corresponding to the drift times given by Eq. (2). Thus the ion beam  $M/Q$  components are displayed as a function of time, with current amplitudes given by the Faraday cup parameters (entrance aperture).

### 3. Deflection Pulse Generator

The deflection pulse generator produces pulses of duration about 100 ns, pulse rise time 20 ns, amplitude from 500 to 2500 V into a matched load of  $50\ \Omega$ , and

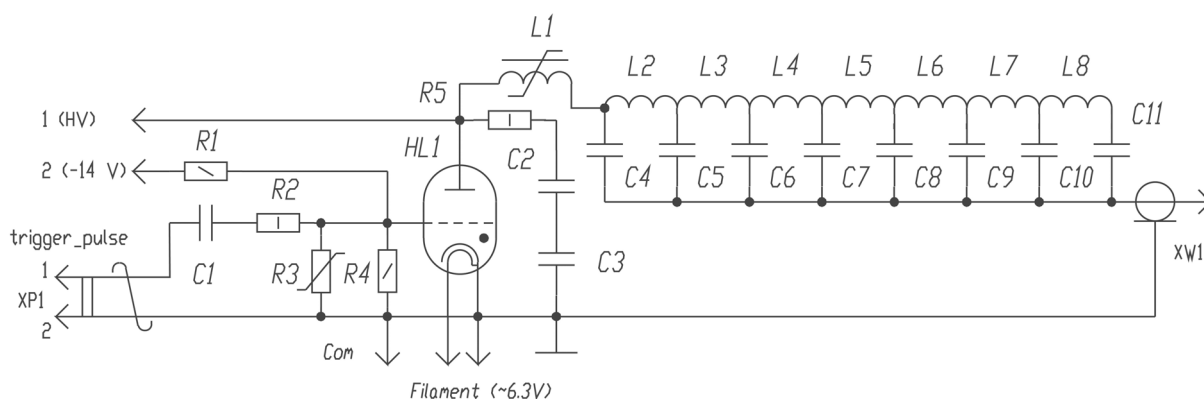


Fig. 3. Schematic circuit of the sub-microsecond pulse generator

is comprised of two main functional units: a high voltage source and a nanosecond pulse former. A schematic circuit of the pulse former is shown in Fig. 3. It consists of a thyatron switch *HL1* (TGI1-100/8) and a pulse forming line with impedance  $50 \Omega$  composed of capacitors *C4*–*C11* (100 pF) and inductors *L1*–*L8*. The thyatron is placed inside a metal cylinder so as to minimize the overall stray inductance in the pulse forming circuitry. Capacitors *C2*, *C3* (470 pF), resistor *R5* ( $51 \Omega$ ), and nonlinear inductor form the circuit for peaking the pulse risetime. The nonlinear resistor *R3* is used to limit the voltage spike from the thyatron. A pulse of amplitude up to 400 V and duration  $10 \mu\text{s}$  is applied from a thyatron triggering circuit to connector *XP1*, switching on the thyatron and discharging the pulse line into the load.

The pulse line is charged from a high voltage power supply comprised of a high-frequency converter composed of thyristor *V\_S1*, elements *R1*–*R5*, *C1*–*C6*, *VD1*–*VD3*, *L1*, and transformer *T1* and a high-voltage rectifier used as a voltage-doubler. High stability of the discharge voltage is accomplished by a negative feedback arrangement.

#### 4. Measurement of Ion Beam $M/Q$ Composition

Measurements of ion beam mass-to-charge composition have been performed using a MEVVA-V vacuum arc ion source [7, 13] that has been made and set up as part of an ion implantation facility at the Ege University (Izmir, Turkey) [14]. A typical oscillogram of the current of the time-of-flight Faraday cup signal for Cr ions is shown in Fig. 4. Here the upper trace is the deflection pulse applied to the gating plates, and the lower trace is the ion current to the Faraday cup. Each peak corresponds to a definite value of  $M/Q$  that can be determined from Eq. (2), and in this way the element and charge state corresponding to each peak can be determined. Thus for example the peaks shown in Fig. 4 correspond to Cr ions with charge states from  $1^+$  to  $4^+$ , with a small fraction of  $\text{H}^+$  and  $\text{N}^+$  ions. The fraction of ions of each type is determined by the amplitude of the corresponding peak.

For multiply-charged ions it is important to distinguish between electrical current  $I_{\text{elec}}$  and particle current  $I_{\text{part}}$ . The ions in general carry a charge  $eQ$ , and so  $I_{\text{part}} = I_{\text{elec}}/Q$ . For this reason the charge state distribution and the mean charge state are different according to whether they are expressed in terms of electrical current fractions or particle current fractions. The Faraday cup measures electrical current, and the beam composition determined directly from the oscillogram is referred to electrical current.

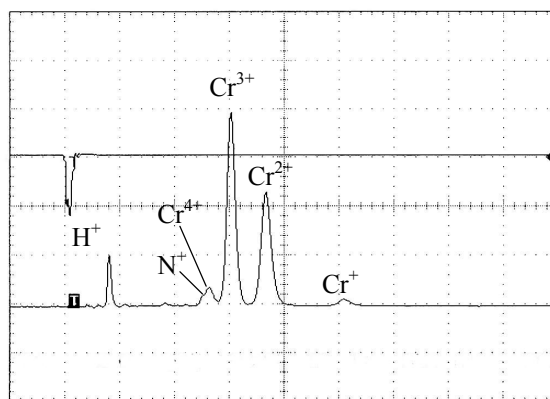


Fig. 4. Mass-to-charge spectrum of a Cr ion beam. Upper trace – gating pulse; lower trace – Faraday cup signal ( $400 \mu\text{A}/\text{div}$ ). Sweep speed –  $1 \mu\text{s}/\text{div}$ ,  $V_{\text{accel}} = 10 \text{ kV}$ ,  $P = 3 \cdot 10^{-5} \text{ Torr}$ ,  $I_{\text{arc}} = 100 \text{ A}$

For given ion source extraction voltage  $V_{\text{accel}}$ , the mean energy of beam ions is given by  $E_i = \langle Q \rangle eV_{\text{accel}}$ , where  $\langle Q \rangle$  is the ion mean charge state. A high mean charge state can often be an important advantage of multiply-charged ion sources such as the MEVVA for applications such as ion implantation when high ion energy leads to high depth of penetration (ion range). The mean charge state expressed in terms of particle current fractions, as is appropriate for ion implantation application where implanted ion number is important, is given by

$$\langle Q \rangle = \frac{\sum_Q (I_{Q(\text{part})} Q)}{\sum_Q I_{Q(\text{part})}}, \quad (3)$$

where  $I_{Q(\text{part})} = I_{Q(\text{elec})}/Q$  is the particle current carried by ions of charge state  $Q$ . (Eq. (3)) can also be expressed as  $\langle Q_{\text{part}} \rangle = \Sigma I_{\text{elec}} / \Sigma I_{\text{part}}$ . According to this expression the Cr charge state spectrum shown in the oscillogram of Fig. 5 corresponds to a Cr ion mean charge state of  $\langle Q_{\text{part}} \rangle = 2.5$  and contains particle current fractions  $f_{\text{part}}(\text{Cr}^+) = 7\%$ ,  $f_{\text{part}}(\text{Cr}^{2+}) = 43\%$ ,  $f_{\text{part}}(\text{Cr}^{3+}) = 48\%$ , and  $f_{\text{part}}(\text{Cr}^{4+}) = 2\%$ . The beam also contains about 30% of gaseous ions (referred to particle current fractions), mainly  $\text{H}^+$  and with a trace of  $\text{N}^+$ , or about 13% of gaseous ions when referred to electrical current fractions.

In some cases the  $M/Q$  values for different ionic species may coincide or overlap. For instance, in the oscillogram of Fig. 4 the  $\text{Cr}^{4+}$  peak is disproportionately broad. Closer inspection shows that a peak corresponding to atomic nitrogen ions,  $\text{N}^+$ , lies very near to the  $\text{Cr}^{4+}$  peak. This should be allowed for in analyzing the charge state distribution. However, the reasonably high resolution of the analyzer makes it possible to uncover such a coincidence in most cases.

The relatively high level of gaseous impurities in the metal ion beam seen here is due to the low pulse repetition rate at which the ion source was operated in these experiments, about 1 pulse per second. It has been shown [15] that the repetitively-pulsed vacuum arc metal plasma generation process is accompanied by greater amounts of gaseous plasma for lower repetition rates. This is because background gas that is adsorbed on the cathode between pulses is desorbed and ionized in the subsequent arc pulse, leading in turn to the formation of a gaseous component to the ion beam and a decrease in the mean charge state of the metal ion component. For these reasons a high pulse repetition rate, say about 10 pps or more, is in general preferred.

## 5. Conclusion

The experimental results demonstrate that a time-of-flight analyzer of the kind we have described can provide a valuable diagnostic for ion beam composition

both as a fundamental research tool and also in technological applications such as for ion implantation. The simplicity, reliability, and low cost of the device add to its attractive features as a worthwhile addition to ion beam instrumentation.

## References

- [1] I.G. Brown (Ed.), *The physics and technology of ion sources*. New York, Wiley, 1989.
- [2] M.D. Gabovich, *The Physics and Engineering of Plasma Ion Sources*, Moscow, Atomizdat, 1972.
- [3] P.M. Schanin (Ed.), *Charged Particle Sources with Plasma Emitter*, Ekaterinburg, Nauka, 1993.
- [4] A.A. Sysoev, *The Physics and Engineering of Mass Spectrometry Devices and Electromagnetic Setups*, Moscow, Energoatomizdat, 1983.
- [5] I.G. Brown, J.E. Galvin, R.A. MacGill, and R.T. Wright, *Rev. Sci. Instrum.* **58**, 1589 (1987).
- [6] B.H. Wolf (Ed.), *Handbook of ion sources*, Boca Raton, FL, CRS Press, 1995.
- [7] I.G. Brown, *Rev. Sci. Instrum.* **65**, 3061 (1994).
- [8] S.P. Bugaev, A.G. Nikolaev, E.M. Oks, P.M. Schanin, and G.Yu. Yushkov, *Rev. Sci. Instr.* **65**, 3119 (1994).
- [9] A.S. Bugaev, V.I. Gushenets, A.G. Nikolaev, E.M. Oks, and G.Yu. Yushkov, *Russian Physics Journal* **43**, 105 (2000).
- [10] B.H. Wolf, H. Emig, D. Rueck and P. Spaedke, *Rev. Sci. Instrum.* **65**, 3091 (1994).
- [11] I.I. Artobolevskii, *Mechanisms in Modern Engineering V. II*, Moscow, Nauka, 1971.
- [12] M. Kaminskii, *Atom and Ion Collisions at the Metal Surface*, Moscow, MIR, 1967.
- [13] I.G. Brown, *IEEE Trans. Plasma Sci.* **21**, 537 (1993).
- [14] A. Oztarhan, C. Bakkaloglu, I. Brown, G. Watt, P. Evans, E. Oks, A. Nikolaev, and Z. Tek, "Surface and Coating Technology", *Proceed. of SMMIB'03* (in publish).
- [15] G.Yu. Yushkov and A. Anders, *IEEE Trans. Plasma Sci.* **26**, 220 (1998).